CONTROL OF BREATHING ATMOSPHERES USING POTASSIUM SUPEROXIDE: AN ENGINEERING ANALYSIS, PHASE II

by

Mark G. White
Union Oil Assistant Professor
School of Chemical Engineering
Georgia Institute of Technology
Atlanta, GA 30332

under

N00612-79-D-8004
HR-49

between

Naval Coastal Systems Center
Panama City, FL 32407

and

Georgia Tech Research Institute
Georgia Institute of Technology
Atlanta, GA 30332

April 15, 1983

ABSTRACT

Potassium superoxide was characterized for surface area, purity, and reactivity towards a moisture-laden helium stream at room temperature and for pressures to 11.5 atm. The surface area measurements show the superoxide is a low surface area material (1-2 m^2/g) showing very little internal pore volume. The technique for determining the purity disagreed with the manufacturer's claim for nearly 99 wt% purity; however, these results are in harmony with those of earlier investigators for a "commercially" obtained superoxide of potassium (70-80 wt% KO_2). We are presently reassessing our technique for measuring KO_2 purity to rationalize the differences in our reported value and those reported by the vendor (MSA, Corp.)

The kinetic results showed three regimes for the time transients in the effluent concentrations: an induction period, a relatively high reaction rate region, followed by a region of relatively low reaction rate. The relatively high reaction rates were attributed to the intrinsic reaction rate of a fresh KO_2 surface not hindered by a product crust. The lower rate was attributed to a diffusion hindered mechanism. The small particles, ca 335 micron diameter, showed a long duration before the diffusional mechanisms controlled the rates; however, even the small particles showed some diffusional effects at high pressures. The diffusional effects at high pressures for the small particle were to shorten the duration of the truly kinetic regime and to lengthen the duration of the total test; the same is true for the large particles at pressure. The pressure effect to 11.5 atm for the intrinsic reaction rate regime is neglible; in fact, one could say the high pressure rate constants may be slightly larger than the low pressure rate constants. There is no question that increasing the pressure does decrease the oxygen production rate for the large particles (2190 micron, diameter) in the diffusion control regime, whereas the small particles do not show such a deleterious effect upon O_2 evolution rate for increasing total pressure. Increasing the particle size at constant pressure does have the expected effect: decreasing rates of oxygen evolution and water in the diffusion control regime and only minimal effect upon the rates of O_2 production in the truly kinetic controlled regime.

A quick comparison of the performance of a pipe flow reactor vs the gradientless reactor show the rates of O_2 production to be nearly equal; however there was more scatter in the pipe flow reactor data than for the gradientless reactor data. While the pipe flow reactor was nearly isothermal we did note the temperature of the bed was slightly higher (about 4 K) than the corresponding tests in the Berty

reactor. It is also obvious to us that care must be used in making direct comparisons between the data from the two radically different reactors. While our pipe reactor did not exhibit significant axial temperature gradients we speculate such gradients will change drastically when one increases the pressure in such a reactor at constant actual space velocity. The effect upon observed reaction rates for such a change in temperature profile will be profound!

A comparison of our data with those of Kunard and Rodgers show our kinetic controlled data to be about ½-1 order of magnitude higher in O_2 evolution rates and the diffusion controlled data is 20% higher than the data of Kunard and Rodgers. It must be noted that the literature data were for one atmosphere whereas our data were for low and hyperbaric conditions (to 11.5 atm).

CONTROL OF BREATHING ATMOSPHERES USING ALKALI METAL SUPEROXIDES: AN ENGINEERING ANALYSIS, PHASE II

By Mark G. White, Union Oil Assistant Professor
School of Chemical Engineering
Georgia Institute of Technology

Introduction

Chemical systems for the revitalization of breathing atmospheres have been employed successfully in the life support systems of marine and space vehicles for more than a decade [1,2]. In one configuration these chemical systems, namely alkali metal superoxides, provide oxygen and remove some carbon dioxide as part of a closed-cycle life support system [3]. These superoxide compounds would appear to be likely candidates as air revitalizing chemicals in a one-man back-pack life support system operating in the hyperbaric environment of marine deep diving. For the design of such life support apparatus, the hyperbaric kinetics of the air revitalization reactions with the superoxide must be established since the previously published data report the kinetics at one atmosphere pressure [4-8]. Moreover, the sample superoxides must be carefully analyzed for purity and specific surface area such that correlation of reactivities between samples may be affected. Finally, there is a need to determine these hyperbaric kinetics in the absence of mass transfer disguise mechanisms and to show the characteristic time as a function of reaction conditions at the onset of such disguise mechanisms, which are known to occur as the chemical is consumed.

In this report we will show the means to characterize potassium superoxide for purity and specific surface area, describe the gradientless, hyperbaric reactor used in the data collection, discuss the pertinent data reduction techniques, report the rate data for the simple hydration of potassium superoxide as function of pressure, and discuss these data in the light of data reported in the literature.

Background

Stull and White [9] review the literature of air revitalization compounds and show potassium superoxide to be the chemical of choice for use in the life support systems of the present technology. Our study indicates all the existing kinetic data of air revitalization over KO_2 may show diffusional effects to some extent. Moreover, the temperature response of these data (Arrhenius Law Activation Energies) is complicated when water and carbon dioxide are present together in the reaction mixture [10].

With the exception of one report [11], no kinetic data have been published for the hyperbaric air revitalization reactions over KO_2. Ducros [11] shows only semi-quantitative data to support the constant reactivity of KO_2 with increasing

pressure. He shows the rates of O_2 evolution at 4 bar (3.95 atm) and at 31 bar (30.6 atm) are sufficient to maintain oxygen partial pressures of 840 milli-bar and 400 milli-bar, respectively, in an enclosure for two human subjects over time periods to 20 hours. An 8 kg charge of KO_2 in two separate cartridges was used in the twenty hour test at 31 bar. No further details were given on the canister operating conditions. These rather sketchy data lead us to measure the hyperbaric kinetics of a well-characterized KO_2 sample in a gradientless reactor designed for such tasks.

There is not a clear determination of the characteristic time for the onset of diffusional limitations to the observed reaction rate; however, several authors report qualitative transients in the rates of oxygen evolution, water absorption, and carbon dioxide scrubbing [4,7]. The transients in the reaction rates will influence the design and control of the chemical life support system insofar as the oxygen production rates must equal the human demand. Whereas the consequences of inadequate chemical oxygen production are obvious, oxygen over-production can have a serious negative impact on the human, as well.

Characterization of the KO_2 has been restricted to purity, porosity, particle size, and density [10]. We could find no reports commenting specifically on the surface area and pore size distribution of the superoxides. The air revitalization reactions occur at the gas-solid interface resulting in the evolution of gaseous oxygen and the formation of solid product crusts of KOH, $KHCO_3$, K_2CO_3 and the associated hydrates. Without question the global reaction rates of the KO_2 sample depend upon the available reactive surface area (not to be confused with the external geometric area of the particles) and the density of reactive sites on the surface. Changes in the surface alone for constant active site density will influence the observed reaction rates. When diffusive mass transfer controls the reaction rates, the pore size distribution will affect the observed rates. "High" surface area solids (about 100 m^2/g) will show smaller diameter pores on the average than "low" surface area solids (about 10 m^2/g) assuming unimodal & normal pore size distributions [12]. Thus, high surface area solids should exhibit a strong tendency for diffusional limitations on the rates at short reaction times. With these thoughts in mind we show characterizations of the KO_2 for purity and specific surface are in order to properly interpret the observed reaction rates.

Approach

For the application of a one-man back-pack in marine deep diving, the life support system must accomodate the varying demands of oxygen consumption, carbon dioxide release, and heat demand as the diver experiences differing work loads, changing ambient temperature and pressure. According to the present technology

the chemical revitalization of the breathing atmosphere using canisters of KO_2 in contact with the exhaled gases driven by human respiration is the technique of choice. The design of KO_2 chemical canisters to serve such a closed life support system requires the proper model for the canister and the intrinsic kinectic data for the model. Stull & White [13] describe one steady-state canister model which requires a knowledge of the air revitalization kinetics free from mass transport disguise mechanisms. They show the limitations of this model for predicting long term canister performance (greater than 5 hours for KO_2 loadings of 2 kg) and recommend the development of unsteady-state models to predict the performance of a KO_2 bed to include consumption of the chemical. These unsteady-state models require a knowledge of the time transients of the KO_2 reactivity as the rate governing mechanism changes from the intrinsic kinetics to diffusion control at the pressures & conditions to be expected for the deep diving environments.

Reaction Kinetics & Transition to Diffusion Control. This study will describe the rates of oxygen evolution and water absorption as a function of temperature, reactant concentrations, total pressure, and time. These time dependent kinetics will be established in a vessel where the gaseous reactor volume is well-mixed and receives a gaseous feed at constant conditions (temperature, pressure, concentration, and volumetric flowrate). The solid KO_2 is placed within the reactor as a shallow fixed bed; the high internal recycle flow of the gases ensure the conversion of reactant per pass is very small whereas the conversion of the inlet gas may be finite. The solid KO_2 will experience a transition from kinetic reaction rate control to diffusional control as the product crusts build; this transition in governing mechanism is made manifest by a change in the reactor effluent concentrations with time.

This gradientless reactor has been used in determining the reaction rates over heterogeneous solids [14]; these rates are determined from a knowledge of the reactant concentrations at the inlet, outlet and the reactor space velocity at steady-state operating conditions. One unique characteristic of this reactor is the ability to establish well-mixed conditions within the reactor at fixed space velocities; unlike the fixed-bed "pipe" reactor, external gradients between the heterogeneous phases can be minimized at will by changing the internal recycle flow at constant overall space velocity.

We propose a series of tests at several space velocities to define the initial rates as a function of inlet conditions for several total pressures

between 0.101 to 1.2 MPa. Moreover, we shall calculate rates as a function of time from the data of concentrations (inlet/outlet) versus time. These rate versus time data will describe three distinct regimes: an induction period for which the reaction rates will increase, an intrinsic reactivity period showing high rates, and diffusion limited regime showing lower rates. It is not possible for us to characterize the two reaction regimes as strictly steady states since the reactivity of the superoxide should change continuously as the product crusts accumulate. In practice, pseudo-steady states may be observed. The time for which a change in the pseudo-steady rate is observed will be ascribed to a change in the rate controlling mechanism.

Characterization of the KO_2. Early work shows the variable reactivity of the potassium superoxide [10]. Since the reaction occurs at a gas-solid interface, the specific surface area of the solid is important to determining the overall reaction rates. We propose to measure the surface area of the superoxide by the BET method [12] to describe the potassium as low or high surface area. Additionally, we will characterize the KO_2 content of the sample by thermally decomposing it and measuring the amount of oxygen evolved.

Experimental

Reactor. A 350 ml (approximately) Berty reactor, fabricated by the Autoclave Engineers, Co. was installed in a flow system to allow for continuous monitoring/control of the gas volumetric flowrate through the device. Such control was affected by two Matheson flowmeters/controllers (Model 8249) for a hydrogen/helium stream and a carbon dioxide stream; the mass flow controllers were calibrated for service up to 1.22 MPa (12 atm) and room temperature (300 K). Introduction of water to the system of known and constant concentration was accomplished by quantitative conversion of the hydrogen/helium stream over a packed bed of CuO at 523 K. This hydrogen converter contained a sufficient weight of CuO to completely convert the hydrogen for all the reactant gas space velocities of this study. Gas phase temperature/humidity was adjusted prior to entering the Berty reactor by a stainless steel coil heat exchanger. Gaseous reaction temperatures within the Berty reactor were measured prior to and just after the KO_2 bed by an Omega Engineering Model 199 temperature indicator attached to Type K (chromel-alumel) thermocouples. Reactor pressure is regulated by a Tescom pressure regulator rated to 250 psig (1.8 MPa); subsequent pressure reduction to the continuous process analyzers was achieved in a Matheson regulator (model 3473).

Gas Analysis. Three small streams were withdrawn from the main reactor effluent stream for analysis of the oxygen concentration (AEI Model S-3A), carbon dioxide concentration (Beckman Model 865-X), and water concentration

(Beckman Model 865). Since the KO_2 reaction is expected to show unsteady-state behavior, continuous process analyzers were necessary to define the concentration versus time behavior. Traces from the analyzers were recorded on single & double pen recorders (Linear Instruments & OmniScribe 5000).

Gas Purification. High purity oxygen (Selox, Inc., 99.95 mole %) was dried over a Matheson drying unit (Model 450). Hydrogen/helium mixtures, prepared and analyzed by the Union Carbide Co., were subjected to a Matheson De-Oxo unit (Model OR-10) and then dried by a Matheson drying unit (Model 450). Bone Dry grade carbon dioxide (Union Carbide Co.) was dried over a drying unit filled with Drierite.

Specific Surface Area. Specific surface areas of the KO_2 were determined by krypton physisorption at 77 K in a Micromeritics Digisorb 2600 automatic surface area analyzer. Samples were evacuated at 75 C (348 K) for 30 minutes prior to analysis.

KO_2 Purity. The purity of the KO_2 was determined from the moles of O_2 evolved during thermal decomposition to K_2O_2; purities of the unknown sample may be estimated by measuring the moles of oxygen evolved at a temperature characteristic for the thermal decomposition to occur by the following equation

$$2\ KO_2 + \text{heat} = K_2O_2 + O_2 \qquad (1)$$

The moles of oxygen evolved are used to calculate the weight of superoxide in the original sample; this weight is compared to the original sample weight to give the percent purity.

A thermal gravimetric analysis (TGA) will yield both the temperature "profile" for the decomposition to identify the proper decomposition temperature and the moles of oxygen evolved. A Perkin-Elmer TGS-II system with a System IV microprocessor was used to thermally decompose the sample. As the sample was heated from room temperature to 475 C (748 K) the weight of the sample decreases showing the evolution of gaseous oxygen from the superoxide. From this weight change, the moles of O_2 is calculated eventually allowing the purity determination. Care must be used to define the heating program which will ensure the final product is the peroxide and not the oxide. Pure sodium peroxide is also decomposed in the same device to show the minimum temperature for which the peroxide is decomposed. The spectra of the weight vs. temperature curves for the superoxide/peroxide are compared to determine if any peroxide is present in the original sample and to ensure the final product is K_2O_2.

Calibration of the instrument was accomplished by thermal decomposition of reagent grade potassium bicarbonate and sodium bicarbonate. These solids were chosen since we knew the purity of each and these solids evolved gaseous products

(water and CO_2) when heated. Examples of the weight (W) and time derivative weight (W) traces for sodium and potassium bicarbonate are shown in Figures 1 & 2 . These traces show how the weight changes with decomposition temperature and define the temperature at which the maximum rate of evolution occurs. Also, these curves define the minimum temperature for which the decomposition is complete. The large negative peak in the W trace defines the thermal decomposition of the bicarbonate whereas the smaller peak(s) show the volatization of water from the sample. The identity of these peaks were identified by introducing gaseous water to a sample which had been dried and noting the increase in peak sizes at the temperatures of the small unknown peaks.

The purities of the calibration standards for several tests are reported in Table I. The potassium compound showed a purity of 98.402± 0.142 wt% whereas the sodium compound gave a purity of 99.383± 0.126 wt%. These values are very close to the actual values and the variation of the analyses is small, less than 0.15 wt%.

During these tests we identified a problem in transferring the chemical to the device; water was "picked" up by the sample. Since the superoxide is very sensitive to water contamination, it was necessary to devise a dry transfer technique for loading the superoxide into the TGA. This problem was solved by coating the superoxide with very cold, dry carbon dioxide such that a crust of CO_2 was formed on the KO_2 to isolate it from the ambient air during the transfer from the dry environment to the TGA. Once inside the TGA, dry nitrogen was used to purge the wet air from the device before the solid CO_2 sublimed. The sample was allowed to warm to room temperature before the analysis was started.

This technique was tested with the bicarbonate samples used as the calibration runs. The diagnostic for determining the success of this technique was the small water peaks at 100 C (approx.). The samples were dried in the TGA to remove the water peaks and weighed. These samples were coated with the cold CO_2 and transferred to the TGA for analysis. The samples of $NaHCO_3$ did not show any accumulation of H_2O for this dry transfer, see Fig. 1 ; the purity of these coated samples was 99.316± .12 wt

Experimental Procedures. Since the potassium superoxide is both hygroscopic and deliquescent, it must be handled in a dry environment at all times. Sample preparation, which includes weighing and transfer to the reactor, was accomplished in dry boxes flushed with dry helium. The shipping container was opened in one dry box where the proper amount of superoxide was sieved & loaded into a sample holder. This sample holder was put in dessicator for transfer into another dry box attached to the top of the Berty gradientless reactor. The sample holder was simply dropped into the reactor and the top flange of the reactor was bolted down.

The reaction rate for the hydration of the superoxide was determined as a

function of water partial pressure, total pressure and time. Previous work [4,7] shows the simple hydration of KO_2 to follow first order kinetics for the reactant water; however, there has been no definitive study of the pressure effect on the kinetics. Two partial pressures of water (611 Pa & 3.16 kPa; dewpoints = 273 K & 298 K, respectively) were chosen to characterize the influence of water partial pressures; the reactor pressure was varied between 0.101 to 1.22 MPa.

We anticipate the reaction rate to vary continuously (see Theory Section) as the moist helium is contacted with the superoxide. For the present case, the concentration vs. time data of the reacting KO_2 must be corrected for any minor mixing effects not associated with the completely mixed Berty reactor using the concentration response to a step input to the reactor in a non-reactive mode containing a volume of inert glass equal to the volume of KO_2 used during the reacting tests. This non-reactive tracer test was repeated for each set of conditions we report for the reaction tests.

The agitation of the Berty reactor was set to ensure complete mixing of the gas within the reactor and to minimize concentration gradients between the gas phase and the solid phase. Replicate tests to measure reaction rates for fixed space times while increasing the agitator speed ensured that external mass & heat transfer mechanisms did not limit the observed reaction rates.

Theory

The hydration of potassium superoxide to yield oxygen necessarily involves a solid product, KOH. As the reaction proceeds, each granule of superoxide shows a shrinking core of reactive KO_2 surrounded by an inert layer of KOH. At some characteristic time, t_d, the diffusion rate of reactant water through the inert crust will influence the observed reaction rate. Eventually, the granule will no longer yield oxygen at a satisfactory rate and the chemical is said to be exhausted. This transient nature in the reaction rate may dictate special precautions in analyzing the data from the Berty reactor;to evaluate the influence of this time varying rate, a reactor model was developed for the case of step input function in the gas phase.

Model. The usual assumptions will be used for the Berty reactor operating at a constant pressure, temperature, and inlet gas volumetric flowrate.

1) Gas phase is perfectly mixed
2) Volume expansion/contraction effects can be neglected
3) Concentration of gas at the outlet is equal to the concentration within the reactor
4) External gradients in temperature/concentration are small
5) The input concentration to the reactor, $a(t) = a_o\, S(t)$ where $S(t)$ is the unit step function.

The appropriate conservation equations for each gas phase specie is

$$V_g \, dc_i/dt = Q\, a(t) - Q\, c_i - k\,(c_i - c_i^*) \qquad (2)$$

$$\& \quad W_s \, r_i(t) = k\,(c_i^* - c_i) \qquad (3)$$

Adding these two equations gives

$$V_g \, dc_i/dt = Q\,[\, a(t) - c_i \,] + W_s \, r_i(t) \qquad (4)$$

This equation (4) may be rearranged to give the rate explicitly as a function of the inlet, outlet concentrations, reactor volume, volumetric flowrates, and superoxide loadings.

$$r_i(t) = [Q/V_g \,[\, c_i - c_o \,] + d/dt \,[\, c_i - c_o]] \,/\, W_s \qquad (5)$$

Thus, the rate as a function of time is determined by the difference of the inlet/outlet concentrations divided by the space time (V_g/Q) plus the the time derivative of this concentration difference. When the concentrations at the effluent change very slowly with time such that the second term is small when compared to the first term in Eq. (5) then this equation reduces to the familiar steady state solution to the well-mixed flow reactor. A series of tests having smaller values of the space time will yield a family of rate versus time curves; as the space time approaches zero, these curves will tend to an asymptotic curve of rate vs. time for the case of zero conversion, hence for the inlet conditions. This procedure may be repeated for different inlet conditions to elucidate the rate as a function of inlet partial pressures, inlet temperature, and time.

The characteristic time for the onset of diffusion limitation should be apparent as the rates will decrease with time and the apparent reaction order will tend towards (n+1)/2 where n is the intrinsic order of reaction [21]. In the limit of extreme diffusional control, all observed rates will be first order in accordance to the "reaction order" of the diffusion process.

The Shrinking Core Model. From several models of gas-solid reaction with reactant diffusion past a product crust [19], we have chosen the shrinking core model as a first attempt to characterize the KO_2 hydration reaction. This model assumes the reactant B (KO_2) to be non-porous (or porous but severely diffusion limited) such that the reaction occurs on the outer, reactive surface. As the reaction proceeds, a product crust (KOH + hydrates) advances into the pellet. A distinguishing characteristic of the shrinking core model is the reaction occurs only at the interface between the unreacted core (KO_2) and the solid product crust (KOH + hydrates).

The two-phase reaction to be modeled is

$$A(g) + b\ B(s) = e\ E(g) + f\ F(s)$$

where

A = water; B = potassium superoxide; E = oxygen; & F = KOH

b = 2; e = 3/2; & f = 2

We presume the potassium superoxide pellets are nearly spherical having an initial radius of r_s. As the reaction proceeds the interface between the product F and the reactant B is characterized at the radius r_c. The concentration of reactant A in the bulk phase, external surface, and at the interface is denoted by the subscripts b, s, and c, respectively.

At pseudo-steady state, the rates of mass transport of A to the external surface, through the product curst, and the reaction rate for the first order, irreversible hydration reaction are equal. These ideas expressed in the lingo of mathematics are as follows:

$$-dN_A/dt = 4\pi r_s^2 k_m [c_{A,b} - c_{A,s}] = 4\pi r_c^2 D_e\, dc_A/dr|_{r_c} = 4\pi r_c^2 k\, c_A|_{r_c}$$

A solution to the diffusion of A from r_s to r_c gives

$$c_A|_r - c_A|_{r_c} = [c_A|_{r_s} - c_A|_{r_c}]\ (1-r_c/r)/(1-r_c/r_s)$$

Wen gives the final solution to these differential equations as the time for complete conversion of the solid B (t) in terms of the initial radius of the particle (r_s), the kinetic rate constant (k), the mass transport coefficient (k_m), the effective diffusivity (D_e), the molecular weight of B (M_b), the solid particle density of B (ρ_b), the bulk concentration of A ($c_{A,b}$), and the stoichiometric coefficient of B (b). We present here the case where the mass transport coefficient, k_m, is much larger than the diffusional and kinetic parameters. This assumption is justified by the experimental procedure which allows us to eliminate mass transport effects within the gradientless, Berty reactor.

$$t = [1 + k\ r_s/6\ D_e]\ (\rho_b r_s/b\ M_b\ k\ c_{A,b})$$

A series of kinetic experiments may be proposed for which all the experimental conditions are held constant (temperature, pressure, bulk concentration of A) while the initial radius of the pellet is varied. The above equation may be linearized by dividing through by r_s which suggests the experimental data may be plotted as t/r_s vs r_s. The slope of this plot is inversely proportional to the effective diffusivity whereas the intercept is inversely proportional to the kinetic rate constant. The ratio of the slope to the intercept defines the ratio of the rate constant to the effective diffusivity, k/D_e. The data which show no dependence of rate with particle size may be used to elucidate the kinetic rate constant; the data showing such dependence will describe the effective diffusion constant, D_e.

Results—BET Surface Area

Two samples were sent to the Micromeritics Materials Analysis Laboratory (Norcross, GA) for a surface area determination on a Digisorb 2600. As expected, the specific surface area of the KO_2 sample is very low, thus necessitating the use of krypton as the adsorbate. The reported surface area is 1.3 ± 0.8 m^2/g; this determination shows an uncertainty almost equal to the value of the surface area itself. A duplicate surface area determination was commissioned on the same lot of KO_2; the reported area was 2.5 ± 2.2 m^2/g. These powders show a mean particle size of 100 microns which gives an external, geometric surface area of 0.028 m^2/g assuming spherical geometry and a superoxide density of 2.14 g/cc. A comparison of the geometric surface area to the specific surface areas show the KO_2 to have some internal pore structure. This internal pore structure allows for the rates to be limited by pore diffusion of the reactant water past the product crust to the reactive superoxide core.

Results—Purity

The calibration runs using the bicarbonates established the validity of using the thermal decomposition technique to determine the sample purity when the stoichiometry of the decomposition is known. These tests show that care must be exercised in the handling of the sample prior to the decomposition. Pre-decomposition drying of the sodium bicarbonate at temperatures in excess of 125 C (398 K) did cause a small amount of sample to decompose prematurely as indicated by the low purity of entry 4 (Table I) and the larger uncertainty in the reported purity (± 0.71 vs ± 0.14 wt%). Similar precautions for the pre-decomposition drying of the KO_2 must also be observed; Bell & Sudhukhan [15] report the onset of KO_2 decomposition to occur at 125 C (398 K) for the reaction to form potassium peroxide They show the decomposition of the superoxide in the TGA to be a superior technique for determining sample purity because the wet technique by Seyb & Kleinberg [16] is not always reliable [17,18].

Sadhukhan & Bell [17] show the weight loss in a dry environment up to 375 C (648 K) is a result of the decomposition of the superoxide to form the peroxide and that none of the peroxide decomposed. They show the purities of the commercial KO_2 to be between 71 and 76 wt% using the TGA technique. We show purities of KO_2 obtained from MSA to be 70.05+ 1.2 wt%. Since this test did not account for any peroxide impurity in the sample, initially, another TGA procedure was developed . In this complimentary procedure, a fresh sample of superoxide was hydrated inside the TGA by a moist nitrogen stream (dewpoint = 0 C). The sample was then heated

in dry nitrogen to 450 C (723 K) at 10 K/min until no further change in the sample weight was noticed and the sample was cooled to room temperature for a final weight determination. If the impurities are assumed to be peroxide and hydroxide, then the weight change upon hydration would give the reactive potassium content. The heating of the hydrated sample to 623 K will convert the final product to KOH (i.e. no hydrates); thus, the weight change reflects only the overall reaction of the peroxide and superoxide originally in the sample to to the final product: KOH. Using the thermal decomposition data together with the hydration data, we report the sample purity as follows: KO_2=70 wt%, K_2O_2 = 7 wt%, and KOH = 23 wt %.

Results— Residence Time Distribution (Table 2)

Tracer studies using a step input of oxygen were performed to document the time constants for the mixing phenomenon within the reactor and for the analyzers. The purpose of these studies was to establish conditions within the reactor which minimize the time constants for the mixing/analysis next to the chemical reaction time constants. When the time constants of the mixing/analysis are much less than the reactive/diffusive time constants, the concentration responses vs time may be used directly without any correction to establish the instantaneous rates of reaction. These criteria are met for the reaction tests involving KO_2 loadings greater than 0.1 gram; the 0.05 gram tests however, do not last a sufficiently long time to decouple the time constants for mixing/analysis from those of the reaction/diffusion. The time constants given in Table 2 are for the return of the oxygen concentration to 99% of its original value; a physical interpretation of these data relates these time constants to that time required for the past history of the reactor to be erased.

Results— KO_2 Hydration in the Berty Reactor for Small Particles (Tables 3&4; E 2-13)

Small particles of KO_2 (40-60 mesh; 420-250 microns) diluted with 470 micron non-porous glass beads were reacted with a water/helium mixture (nearly saturated) at room temperature (294 K) at pressure to 11.5 atm, absolute, in the gradientless Berty reactor. No carbon dioxide was present in the inlet gas in as much as these tests were to establish the kinetics of the simple hydration as a function of total pressure. The volumetric flowrate was varied between 0.55 & 0.8 sl/min. It was of interest to document the outlet oxygen/water concentrations as functions of time on stream; zero time was ascribed to that moment when reacting gases were directed to the dry-He filled Berty reactor containing the dry KO_2.

The pertinent data and calculated results are given in Table 3 for the Berty reactor runs; representative traces of the oxygen/water concentrations are shown in Figs. 5 & 11. All tests show three distinct regimes most clearly defined by the oxygen trace in Fig. 5. The induction period showed the combined effects of mixing/flushing of the reactor together with the initiation

of the reaction(s) to form oxygen. In the 11.5 atm tests the mixing/flushing characteristics show up as an inflection point near the time required to flush 99% of the reactor contents. The kinetic region is clearly described for the low pressure tests (4.17 atm) as a plateau of constant oxygen concentration; this same kinetic region for the 11.5 atm test is given by a broad peak in the oxygen concentration curve appearing after the induction period. Subsequent to the kinetic period is a region showing decreasing concentrations of O_2 with time, perhaps indicative of a diffusion limited process even with these small particles. We report in Table 3 the oxygen/water concentrations in the kinetic control/diffusion (?) control region, the duration of the kinetic control region, and the duration of the diffusion control regime. From these data we may calculate the rates of oxygen production, water absorption using the reactor design equations given in the Theory Section. These reaction rates given in Table 4 and plotted in Figs. 3 & 4 show the effects of total pressure. If one examines the apparent reaction rate of O_2 evolution vs water concentration (Fig. 3) the effect of increasing the total pressure from 4.17 to 11.5 atm is small for both the kinetic and diffusion control regions. In fact there may be reason to say the rate of oxygen production actually may increase for increasing total pressure, but the scatter in the data at both pressures is larger than what one may want (about 20% relative). One indicator of the reliability of these data is the overall material balance (weight recovery) for the oxygen. The moles of oxygen recovered/gram of KO_2 may be calculated from the oxygen concentration vs. time trace. For pure KO_2 the stoichiometric yield of O_2 per gram of chemical is 1.055×10^{-2} moles/g; the values for the Berty reactor tests vary between 0.49×10^{-2} (one test, E-8) to 1.16×10^{-2} moles/g. The average for these tests is 0.88×10^{-2} moles/g. If these samples are not pure superoxide, then the theoretical yield will decrease, e.g. suppose the purity of the sample loaded into the reactor is 80% then the theoretical yield is 0.84×10^{-2} moles/g. We believe the weight recovery of oxygen for these tests is acceptable considering the purity of the samples.

The data of oxygen reaction rates are most easily correlated per total weight of superoxide plus glass; a visual inspection of the superoxide/glass after the run shows the solid potassium compounds to be intimately mixed with the glass beads. When no carbon dioxide has contacted the bed of reactant the mixture of glass and chemical remained granular unlike the pure chemical which fuses into a solid mass with some unreacted chemical apparent at the conclusion of the test. The glass/chemical mixture could be easily contained in a bed and the porosity of this reacted/exhausted bed seemed to be much higher than the same bed of

exhausted chemical without the glass beads. For these tests we used a glass/chemical ratio of 10-20. It seems as though the partially hydrated chemical does coat the outer surface of the glass beads, but more work is required to document this claim.

The rates of water absorption given in Table 4 decrease by almost 50% when the total pressure is increased from 4.17 to 11.5 atm. We note the water absorption reactions continue for a time long after the O_2 evolution reaction ceases, and the rates of water absorption are much larger than those predicted by stoichiometry to evolve the observed amount of oxygen.

Results—KO_2 Hydration in the Pipe Reactor for Small Particles (Tables 3 & 4; E-14-19)

Small particles of KO_2 (40-60 mesh; 420-250 microns) diluted with 470 micron non-porous glass beads were reacted with a water/helium mixture (nearly saturated) at room temperature (294 K) at pressures to 11.5 atm, absolute, in a pipe flow reactor. No carbon dioxide was present in the inlet gas in as much as these tests were to establish the kinetics of the simple hydration as a function of total pressure. The volumetric flowrate was set at 0.642 standard liters/min. The purpose of these tests were to show the effect upon performance for changes in the design of the reactor; the pipe reactor is not the design of choice for a reactor to elucidate reaction kinetics whereas the gradientless reactor is the desired reactor design. These tests will bear out these comments.

As in the Berty reactor three distinct regions are apparent in the traces of concentration vs time (Fig. 7 & 8). The induction time for the pipe flow reactor is obviously shorter than the same in the Berty owing to the differences in the design & volume. The pipe reactor shows much less mixing inside the reactor thus the rise to maximum concentration in oxygen is fast (Fig. 7). The effects of bed stratification in the pipe reactor are most obvious when one considers the transient nature of the oxygen concentration in the effluent (Fig. 7). For the pipe reactor at low pressure (4.17 atm) there is no plateau as was observed for the oxygen response in the Berty reactor at the same conditions (Fig. 5). The duration of the pipe flow tests are much shorter than the duration of the Berty reactor tests at the same conditions; e.g., 1 hour (E-14) vs 3 hours for the Berty reactor (E-6). The change from kinetic control to diffusion control which is obvious in the Berty tests is not so obvious in the low pressure pipe reactor tests. At high pressures, the distinction between kinetic and diffusion control for the Berty reactor tests is equally poor as for the pipe flow reactor (See Figures 6 & 9).

As the total pressure is increased for the pipe flow tests the time on stream for exhaustion increases, the maximum in the O_2 concentration decreases in value and shifts to a longer time (10 minutes @ 4.17 atm vs. 25 minutes @ 11.5 atm). These tests (E-14-E-19) are all at the same standard space velocity thus the shift in position for the peak maximum may be partly explained by a residence time effect for the change in total pressure.

Since it was difficult to distinguish between kinetic and diffusion control in the pipe flow reactor tests, we report only one set of values, under the heading of kinetic, in Tables 3 & 4. It must not be construed that these entries represent truly kinetic numbers, thus we have marked the same with an asterisk (*). As expected the water conversions for the pipe reactor tests are all higher than the corresponding Berty reactor tests. The maximum oxygen concetrations in the pipe reactor tests are all higher than the corresponding values observed in the Berty reactor tests and the run durations are all shorter. These observations are in complete harmony with the differences in reactor design effects between the gradientless/pipe flow reactor. There is more scatter in the "canister" average reaction rates reported for the pipe reactor (Table 4) than what is observed for the kinetic reaction rates reported for the Berty reactor.

Results—Effect of Particle Size (E-2—E-13 and E-20—E-24)

Tests to document the effect of increasing particle size from 40-60 mesh (335 micron) to 8-10 mesh (2190 micron) were conducted in the gradientless Berty reactor at room temperature for pressures of 4.17 and 11.5 atm and for a volumetric flowrate at 0.642 sl/min. The inlet water concentration for these tests was 7500 ppm and the weight c ' 2.0 g ow pressure, large particle tests (E-20,21,24) s e as the low pressure, small particle tests diffusion controlled rates were sli tests (e.g.; compare E-21 to E-6). The d gime for the small and large particles runs hereas the diffusion controlled durations longer than the duration of the same regin 12).

The water uptake is strongly c (See Fig. 12). There seems to be a cons rate as a function of time after the ini n. The initial response after the time he large particle tests show an interesting nutes on stream. The water conversion in e 3) is 4-9% lower for the large particles the corresponding decrease in rates o the large particles in the kinetic con ntrol rates for the large particles are

DISCUSSION OF RESULTS

Choice of a Kinetics Reactor

The choice of the Berty reactor as the device to establish the kinetics is based on our experience with various kinetics reactors. While the pipe flow reactor is simple and inexpensive, the kinetics are difficult to extract from the integral data which may be confused with mass transfer effects, reactor bed by-passing effects, and the spatial gradients in temperature and concentration ("stratified" bed). The Berty reactor does not suffer from these complications. Under the proper experimental conditions, mass transport disguise mechanisms from the bulk phase to the solid surface may be eliminated and the reactor does function under the conditions of no spatial gradients. The data may be manipulated by algebraic equations (at psuedo-steady state) to calculate reaction rates at specified reactant concentrations in the gas phase, thus allowing the kinetics to be specified. In some instances diffusion processes may be distinguished from kinetic processes by a change in the effluent concentration vs. time curve.

Our results of oxygen concentration vs. time (Fig. 5) do show the desirable characteristics of the Berty reactor in favor of the pipe reactor. The low pressure tests in the Berty reactor do clearly establish the kinetic controlled rates and the diffusion controlled rates, such a distinction is not so clear for the low pressure pipe flow reactor tests. The Berty reactor tests show much less scatter in the calculated reaction rates than the pipe flow reactor tests ($\pm$ 20% vs. $\pm$ 34%) and less scatter in the moles of oxygen evolved/g KO_2 ($\pm$ 20% vs. $\pm$ 47%).

These considerations lead us to choose the gradientless Berty reactor to be the experimental device for which we report the kinetics data. We show for comparison data of effluent concentration vs time for the pipe flow reactor such that our data may be compared to that of other groups. From our own data it is obvious that a direct comparison of data from the gradientless and "stratified" bed reactors is not possible (Fig. 5& 7).

BET Surface Area and Purity

The surface area data show the KO_2 to be low surface area material. The extreme spread in the values of the surface area is a result of the curious nature of the physisorption isotherm (Type III) which is very difficult to model. The BET model is really unsuitable for this type of isotherm and we are presently working on a physisorption isotherm which will yield more accurate results for the surface area. It is obvious from the raw data that the KO_2 does not show much pore volume; this result will allow a clear choice of models for the reaction and diffusion.

The purity we report for the KO_2 seems low (about 70% KO_2, 7% K_2O_2, balance KOH by weight). Dr. Maustellar of the Mine Safety Appliance Corp. was contacted

on this matter; he checked the purity of product shipped over the last few months and reported it to be 98-99% KO_2 with no peroxide impurity. These results were corroborated by tests at Rutgers University. Our results, however, are in harmony to those reported by Bell, et al. [17] showing superoxide purities between 70-80 wt% for a commercially available superoxide which we presume to be from MSA, Corp. Thus, our results are in question as to purity. At present we are examining the integrity of the dry boxes, interchange chambers, etc. to explain the low purity of superoxide due to contamination with water. Should that prove negative, we shall next question the integrity of our dry transfer technique for the TGA device. For this report we shall assume the KO_2 is 100% pure with the reservation that it may be contaminated to 70% purity level.

Residence Time Distribution

The results of Table 2 show the characteristic times for mixing within the reactor/analyzer time constants are much smaller than the characteristic times for the intrinsic kinetics; thus, there can be no coupling of the two phenomena. Therefore, the transients observed for the concentrations during the kinetic and diffusion controlled regimes are real and need not be corrected.

Hydration Reactions over Small Particles of KO_2

The initial work with small particles of superoxide which were not diluted with an inert show the characteristic and familiar phenomenon of crusting that has been often reported in the literature with the secondary problem of incomplete utilization of the chemical. One reference [20] shows the beneficial effects upon performance of KO_2 blended with an inert matrix of asbestos. The obvious health hazards associated with the use of asbestos lead us to consider glass beads as the inert matrix material. Mixing the 470 micron glass beads with superoxide particles of nearly the same diameter resulted in a bed which did not show the severe crusting characteristics we observed for un-diluted KO_2 and from a material balance plus visual examination the utilization appeared to be improved for the glass impregnated bed. A word of warning is necessary, for these beneficial effects of mixing glass with the superoxide are proven only for the simple hydration; our initial testing with CO_2 present show the glass mixture will also form the rock hard matrix as does the un-diluted chemical. More work is necessary to document the success of mixing superoxide with glass to affect air revitalization when carbon dioxide is also present in the inlet gas. The glass seemed to provide additional surface area for the chemical as the reaction proceeded; the water conversion data correlated best with residence time based on total weight of glass plus chemical rather than a residence time based on just the weight of the chemical. Additional tests at constant KO_2

loading and variable glass loading are planned to document the beneficial support effects of glass upon the reactivity of the chemical. Post-mortem inspections of the glass/chemical bed showed the potassium compound had spread over much of the glass.

At constant reactor conditions except for reactor total pressure, the rate of oxygen evolution is observed to be constant as the total pressure is increased. It must be remembered these rates reported in this study are not disguised by any mass transport effects which may be operative at high pressure (thus reducing the observed rate). The water absorption rates are observed to decrease as the pressure increases; the cause of the decrease may not be due to any drop in the intrinsic activity but rather is a result of the reactor operating conditions as the pressure is increased. The partial pressure of the water is maintained constant between the test of differing reactor pressure by adding a diluent (helium) as the pressure increases; the diluent causes the amount of water to be scrubbed to decrease since there is a smaller mole fraction of this reactant present in the high pressure tests. We chose to operate the reactor at constant molar flowrate rather than constant actual flowrate between the tests of different pressure.

Our data show two distinct reaction rates for the production of oxygen; a relatively high rate at the beginning of the tests and a relatively low rate later into the run. We have attributed the higher reaction rate to be that given by the intrinsic reactivity of the sample whereas the lower rate is said to be influenced by diffusion of gases through the product crusts. The diffussion controlled rate is between 20-40% of the kinetic controlled rate of O_2 evolution. The low pressure tests show the kinetic controlled rates to persist for a longer duration than the diffusion controlled rates; increasing the pressure to 11.5 atm reverses this trend. It would seem that even the small particles are influenced by diffusional processes to some extent; the subsequent testing of the large particles should shed some light of the diffusional processes. A model of diffusion and reaction will be necessary to properly interpret the data.

The water absorption rates for these tests are one-half to one order of magnitude greater than the oxygen evolution tests; considering the reaction stoichiometry to evolve water by the hydration of superoxide these results show that other hydration reactions are operative such as the hydration of KOH, etc. Our tests show the water absorption reactions to continue long after the O_2 evolution ceases; we did not continue the tests once the oxygen evolution stopped to document the subsequent hydration reactions.

Particle Size Effects

These data show the water absorption is affected by particle size when all other conditions are held constant, both in the kinetic and diffusion controlled regimes. However, the evolution of oxygen is affected deleteriously only in the diffusion controlled regime (See Figs. 4 & 12). One explanation of these results would have the non-oxygen producing reactions showing stronger diffusion limitations than the oxygen producing reactions; hence, that part of the water uptake to supply the oxygen producing reactions does not show the diffusion control as soon as the KOH hydration reactions. Another explanation may be related to the tendency of the small particles to become "supported" upon the glass beads much faster than the large particles. A post-mortem analysis of the small & large particle tests show the potassium compounds from the small particle tests to be evenly distributed on the glass beads whereas the potassium compounds in the large particle tests stay together as large particles and do not spread over the glass beads. The increased area afforded by the glass beads in the small particle tests may account for the increased water scrubbing in these tests.

The relatively constant rates of O_2 evolution between the small and large particle tests at 4.17 atm in the kinetic control region do reinforce our claim that these rates are indeed kinetic rates, not disguised by diffusional effects. However, the increase in pressure to 11.5 atm does cause the oxygen evolution rate to decrease for the large particles over the small particles in the so-called kinetic regime. We must conclude, that the small particles are indeed influenced by diffusional processes even at the onset of reaction. Added proof of this claim of diffusion control of the rates at the high pressure for all particle sizes is given in Figure 13; the time of diffusion (weighted by the particle size, the bulk $[H_2O]$, and the weight of KO_2) is plotted vs. total pressure. A zero slope on this plot means the effective diffusivity (temperature dependent term) is infinite, thus not in control of the reaction; any finite slope means that diffusion influences the reaction to some extent. As shown on the plot the slopes for the three loadings of KO_2 is $2.73 \pm 0.10 \times 10^{-3}$; this slope yields a value of 2.56×10^{-4} atm-cm^2/sec. for D_o. At 11.5 atm, the effective diffusivity is 2.2×10^{-5} cm^2/sec whereas the O_2 evolution rate is 3.8×10^{-3} cc/sec. For this reaction rate the water consumption rate would be 2.5×10^{-3} cc/sec. The diffusion flux of water into the center of the 335 micron particle would be 6.2×10^{-8} cc/sec; thus diffusion would limit the reaction rate (This crude calculation assumed the gradient in concentration of water is given by the bulk water concentration/particle radius. This value would be a lower bound for the actual gradient. Thus the calculation predicts severe diffusional limitations when in fact there may be only some diffusion control).

Comparison of these Data with the Literature.

There are several studies of the hydration of KO_2 from which to choose for a comparison; however, we will show only one such comparison to the data of Kunard and Rodgers [10]. Moreover, we will only examine the rates of O_2 evolution as a function of water concentration at room temperature. To review the Kunard & Rodgers data, the tests were conducted in a flow reactor at room temperature to 60 C (333 K) for various inlet water and carbon dioxide partial pressures. Particle sizes that were investigated included large particles (2-4 mesh) down to small particles (10-20 mesh). They show an 11% increase in the rates of oxygen evolution for small particles over the large particles. It must be noted that the "small" particles of the Kunard & Rodgers study are the same size, approximately, of the "large" particles of this study.

We can identify correlations of O_2 rates from the Kunard and Rodgers study for 2-4 mesh particles, at 25 C (298 K), and for water concentrations to 6.1×10^{-4} M to compare with our data at the same temperature, different pressure (4.17 atm vs 1 atm for K & R study), and for different reactor design. This correlation is plotted on Figs. 3 & 4 to compare with our data. All of the kinetic data regardless of particle size show rates of O_2 evolution much higher than the correlation (about 8-10 times as large); only the diffusion limited, large particle tests at 11.5 atm are close to the correlated data of K & R. If we use the factor established in the study of K & R for correcting their data for particles size effects between 2-4 mesh and 10-20 mesh (i.e. a factor of 1.1 in the rate of O_2 evolution) we have the dotted line on Fig. 4. We see that our data for 8-10 mesh particles, diffusion limited, and at 4.17 atm are about 20% higher than those reported in the K & R correlation.

In summary, we believe our data to be in substantial harmony with those given by Kunard and Rodgers. Further, the data of K & R are most certainly influenced by diffusional effects which were very obvious in our study.

Additional Comments

These tests show diffusional effects to become operative very quickly at the higher pressures such that one does not have to worry about the kinetic rates at all for all practical purposes. Most certainly the chemical will be used as large pellets in the 2-4 mesh range because of pressure drop considerations. This study has shown that diffusion will control the rate of O_2 evolution for particles of size 8-10 mesh and larger at pressure of 11.5 atm. This consequence is a mixed blessing in that we need not be overly concered with measuring the kinetics over wide ranges in pressures, but now must focus our efforts on developing a model for diffusion in a large pellet with a reactive crust. These models are not as mature as the models having

a non-reactive crust. As part of a presently funded contract with the NCSC we are currently developing such a model. Moreover, we are under contract to extend the data base given in this study. The carbon dioxide kinetics are a part of this new contract; to better utilize our time, we will measure the rates with carbon dioxide present all at one time. That is to say, the CO_2 work that was scheduled to be done in this contract will be accomplished as part of the new contract. The same will be done for the activation energy work, the 0 C data scheduled for this contract will be a part of the new contract now currently in effect to measure the rates of O_2 evolution to 200 C.

ACKNOWLEDGMENTS

This project required the services of a number of investigators:

Lt. J. G. Jeffrey O. Stull (USCG) who designed and built the apparatus. He also designed and carried out most of the experimental procedures.

Mr. Andrew H. Drexler who assisted Lt. Stull in the construction phase.

Mr. Steven R. Poehlein who characterized the KO_2 for surface area & purity.

Mr. Jim Hocut who characterized the KO_2 for purity.

Mr. Dave B. Mills who assisted Lt. Stull in the experimental procedure.

We acknowledge the faithful services of these scientists.

REFERENCES

1. Li, Y. S., "A Potassium Superoxide Life Support System for Deep Quest", Biotechnology, Lockheed Missiles and Space Company, Sunnyvale, CA, undated report.

2. Bovard, R. M., "Oxygen Sources for Space Flights", Aerospace Medicine, 31, No. 5, 1960, pp 407-412.

3. Presti, J., H. Wallman, & A. W. Petrocelli, "Superoxide Life Support Systems for Submersibles", Undersea Technology, June, 1967, pp 20-21.

4. Kunard, D. J. & S. J. Rodgers, "Exploratory Study of Potassium and Sodium Superoxide for Oxygen Control in Manned Space Vehicles, N62-1108, MSA Research Corp., Callery, PA, (1962).

5. Ducros, H., "Use of Potassium Superoxide in Closed Circuit Individual Breathing Apparatus", Revue de Corps des Sante Armees, Vol. II, 1970, pp 67-87 (English Translation).

6. Li, Y. S. & others, "Emergency Breathing Apparatus", U. S. Patent No. 3,942,524, March 6, 1976.

7. McGoff, M. J. & J. C. King, "Superoxide Configurations for Atmosphere Control Systems", AMRL-TR-66-167, Aerospace Medicine Research Laboratory, Wright Patterson, AFB, OH, 1966.

8. Melnikov, A. K. & T. P. Firsova, "The Reaction Between Sodium Superoxide and Carbon Dioxide in the Presence of Water Vapor", Russian Journal of Inorganic Chemistry, (English Translation), Vol. 6, No. 6, 1962, pp 633-637.

9. Stull, J. O. & M. G. White, "Air Revitalization Compounds: A Literature Survey", Ocean Engineering Division, Vol 10, pp 33- .

10. Stull, J. O. & M. G. White, "An Engineering Analysis on the Control of Breathing Atmospheres Using Alkali Metal Superoxides, Phase I", Final report delivered to the Naval Coastal Systems Center, Panama City, FL, Jan. 15, 1982.

11. Ducros, H. J. Colin, M. Rio, & Chovet, "Regeneration D'Atmosphere D'Enceintes Closes Par le Superoxyde de Potassium", Revue de Medicine Aeronautique et Spatiale, 45, 1973, pp 193-196 (in French).

12. Brunnauer, S, P. H. Emmett, & E. Teller. J.A.C.S., 60, 309 (1938).

13. Stull, J. O. & M. G. White, "Modeling Potassium Superoxide Canister Performance in Air Revitalization Systems: A Parametric Study", presented to ASME Winter Annual Meeting, Phoenix, AZ, November 16, 1982.

14. Weekman, V. W., "Laboratory Reactors and Their Limitations (Journal Review)", A.I.Ch.E. Journal, 20, pp 833-840.

15. Bell, A. T., & P. Sadhukhan, "The Synthesis of Higher Oxides of Alkali & Alkaline Metal & Earth Metals in an Electric Discharge: Theoretical and Experimental Studies", University of California, Berkeley, August, 1974, (N75-26059).

16. Seyb, E., & J. Kleinberg, "Determination of Superoxide Oxygen", Anal. Chem. 23, 1 (1951).

17. Sadhukhan, P. and A. T. Bell, "Synthesis of Higher Oxides of Potassium in an Electric Discharge Sustained in Oxygen", J. Inorg. Nucl. Chem., 38, pp 1943-1948 (1976).

18. Wood, P. C., J. Wydeven, & E. V. Ballou, "The Preparation of Calcium Superoxide in a Flowing Gas Stream, and Fluidized Bed", presented at Inter-society Environment Systems Conference, San Diego, CA, July, 1980, (ASME: 80-ENas-18).

19. Wen, C. Y.,Ind. Eng. Chem. 60, 34 (1968).

20. Gustafson, P. A., U. S. Patent No. 4,238,464 (1978).

21. Levenspiel, "Chemical Reaction Engineering", 2nd Edition, John Wiley & Sons, (New York), p 490 (1972).

* Drying of the samples in the TGA may have caused some decomposition of the $NaHCO_3$ to occur before the test was started.

TABLE I CALIBRATION OF THE THERMAL GRAVIMETRIC ANALYSIS AND TESTING THE CO_2 ENCAPSULATION

Number of runs	Bicarbonate cation	Encapsulation	Purity, wt%
9	K	no	98.402± 0.142
7	Na	no	99.383± 0.126
2	Na	yes	99.316± 0.118
7*	Na	no	98.669± 0.710

* Drying of the samples in the TGA may have caused some decomposition of the $NaHCO_3$ to occur before the test was started.

TABLE 2 RESIDENCE TIME DISTRIBUTION (RTD) STUDIES TO ESTABLISH THE TIME CONSTANTS FOR MIXING & ANALYSIS

Pressure (atm)	Space Velocity (sl/min)	Time Constants for Mixing and Analysis (min)
1.0	0.642	1.95
4.17	0.642	6.15
6.0	0.642	8.31
9.0	0.642	11.6
11.5	0.642	13.9

Note: The time constants reported here are actually 3 x the space time of the well-mixed reactor where the space time is defined as the gaseous volume of the reactor divided by the volumetric flowrate of the gas at flowing conditions.

TABLE 3 KINETIC DATA FOR THE HYDRATION OF POTASSIUM SUPEROXIDE AT ROOM TEMPERATURE IN VARIOUS [illegible]

Run I.D.	Wt. KO_2 grams	Water Concentrations inlet	outlet (kin)	outlet (diff)	Outlet O_2 Conc. (kin)	(diff)	Vol. Flow sl/min	Water Conv. %	Total Press. (atm)	Weight of Glass grams	Duration of Region Oxygen (minutes) (kin)	(diff)
E-1	Aborted — No data reported											
E-2	0.100	7500	2500	2900	392	75	0.550	67	4.17	2.0	100	20
E-3	0.100	7500	3700	4100	350	140	0.642	51	4.17	2.0	98	30
E-4	0.100	7500	3100	3600	284	110	0.800	59	4.17	2.0	66	90
E-5	0.100	7500	3800	4700	318	140	0.550	48	4.17	2.0	66	54
E-6	0.100	7500	3650	3650	335	160	0.642	51	4.17	2.0	66	48
E-7	0.200	7500	3600	4100	320	125	0.642	52	4.17	2.0	174	30
E-8	0.051	7500	3400	3900	310	150	0.642	55	4.17	2.0	7	43
E-9	0.103	2600	700	800	340	140	0.642	73	11.5	2.0	28	136
E-10	0.201	2600	700	800	370	135	0.642	73	11.5	2.0	46	230
E-11	0.051	2600	720	1050	300	108	0.642	72	11.5	2.0	36	90
E-12	0.100	2600	700	950	400	160	0.642	73	11.5	2.0	28	131
E-13	0.201	2600	700	900	450	202	0.642	73	11.5	2.0	53	198
E-14	0.100	7500	700	—	1100*	—	0.642	91	4.17	2.0	60*	—
E-15	0.100	7500	700	—	810*	—	0.642	91	4.17	2.0	47*	—
E-16	0.100	2600	100	—	350*	—	0.642	96	11.5	2.0	156*	—
E-17	0.100	2600	250	—	500*	—	0.642	90	11.5	2.0	163*	—
E-18	0.100	2600	250	—	300*	—	0.642	90	11.5	2.0	138*	—
E-19	0.100	2600	550	—	800*	—	0.642	93	4.17	2.0	52*	—
E-20	0.100	7500	4000	4800	350	120	0.642	47	4.17	2.0	56	78
E-21	0.100	7500	4000	4900	320	89	0.642	47	4.17	2.0	62	154
E-22	0.100	2600	1450	1900	250	40	0.642	44	11.5	2.0	90	3840
E-23	0.100	2600	1250	2050	300	95	0.642	52	11.5	2.0	72	terminated
E-24	0.100	7500	5000	6600	400	110	0.642	33	4.17	2.0	78	"
E-25	0.100	2600	2000	2150	260	110	0.642	23	4.17	2.0	72	108
E-26	0.100	2600	2000	2200	230	90	0.642	23	4.17	2.0	72	144

TABLE 4 KINETIC DATA FOR THE HYDRATION OF POTASSIUM SUPEROXIDE AT 25°C

Run I.D.	Oxygen Production Rates (moles/min) x 1000000 (kin)	(diff)	Moles of Oxygen Evolved/g KO_2 moles/g x 100	Total Pressure (atm)	Duration of Regions Water (minutes) (kin)	(diff)	Water Absorption Rates (moles/min) x 10000 (kin)	(diff)
E-1	Aborted — No data reported							
E-2	9.6	1.8	0.996	4.17	200	492	1.23	1.12
E-3	10.0	4.0	1.10	4.17	100	152	1.09	0.97
E-4	10.1	3.9	1.02	4.17	140	116	1.51	1.39
E-5	7.8	3.5	0.70	4.17	144	52	0.88	0.72
E-6	9.6	4.6	0.85	4.17	378	—	1.10	—
E-7	9.2	3.6	0.86	4.17	174	44	1.10	0.98
E-8	8.9	4.3	0.49	4.17	80	36	1.19	1.04
E-9	9.8	4.3	0.82	11.5	80	108	0.55	0.52
E-10	10.6	3.9	0.69	11.5	124	184	0.55	0.52
E-11	8.8	3.2	1.16	11.5	42	162	0.54	0.44
E-12	11.4	4.6	0.91	11.5	56	102	0.55	0.47
E-13	12.9	5.8	0.91	11.5	128	122	0.55	0.49
E-14	14.3*	—	0.86	4.17	110*	—	—	—
E-15	11.8*	—	0.56	4.17	70*	—	—	—
E-16	14.4*	—	2.25	11.5	168*	—	—	—
E-17	4.6*	—	0.74	11.5	160*	—	—	—
E-18	6.1*	—	0.76	4.17	168*	—	—	—
E-19	14.8*	—	0.84	11.5	96*	—	—	—
E-20	10.0	3.4	0.83	4.17	13	196	1.00	0.75
E-21	9.7	2.6	0.97	4.17	16	268	1.00	0.77
E-22	7.2	1.1	1.13	11.5	-	-	0.33	terminated
E-23	8.6	2.7	1.14	11.5	-	-	0.39	"
E-24	11.5	3.2	1.65	4.17			0.71	"
E-25	7.5	3.2	0.87	4.17	148	40	0.17	0.13
E-26	6.6	2.6	0.84	4.17	96	148	0.17	0.11

FIGURE 1 THERMAL DECOMPOSITION SPECTRUM OF $NaHCO_3$

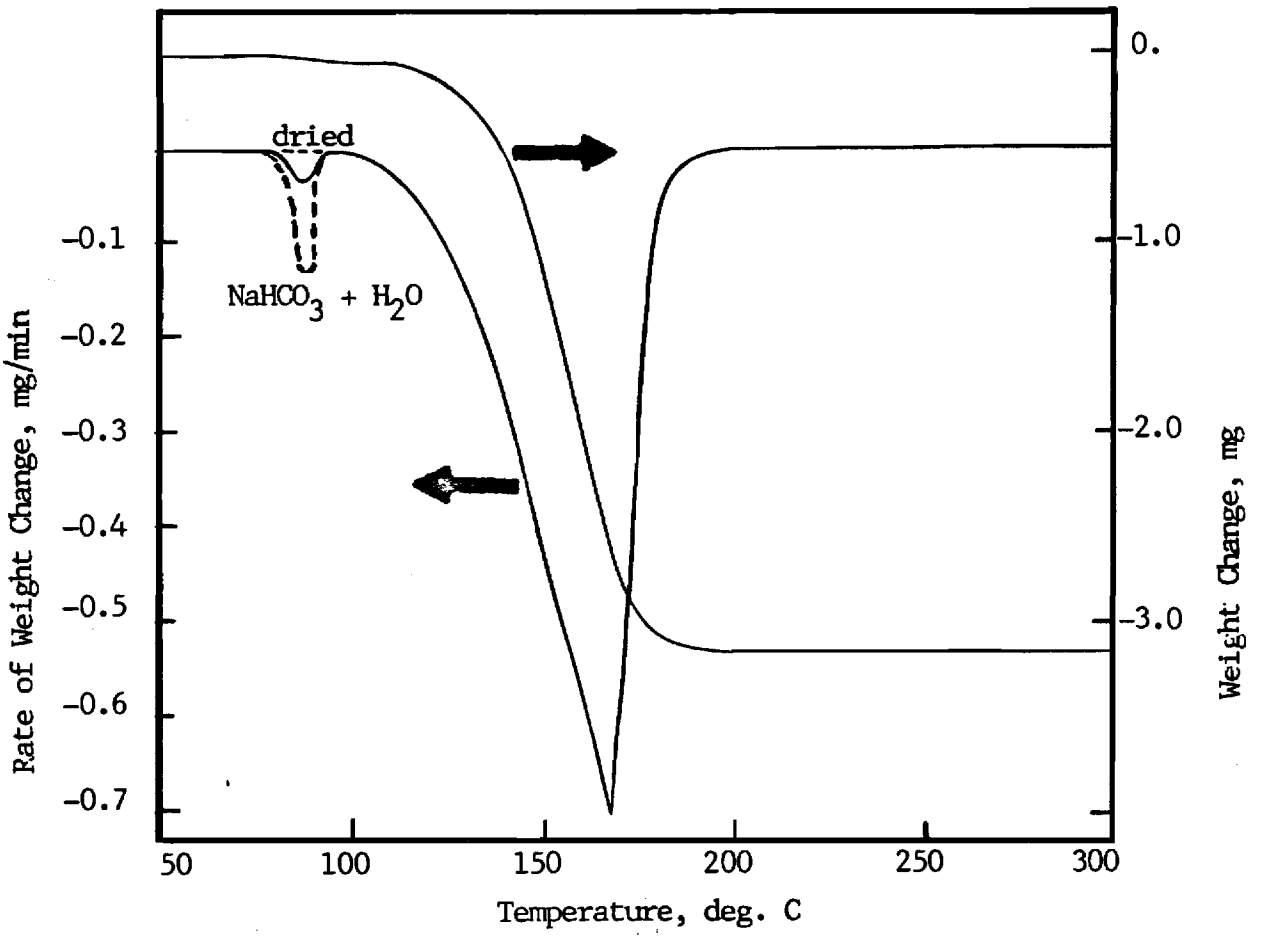

FIGURE 2 THERMAL DECOMPOSITION SPECTRUM OF $KHCO_3$

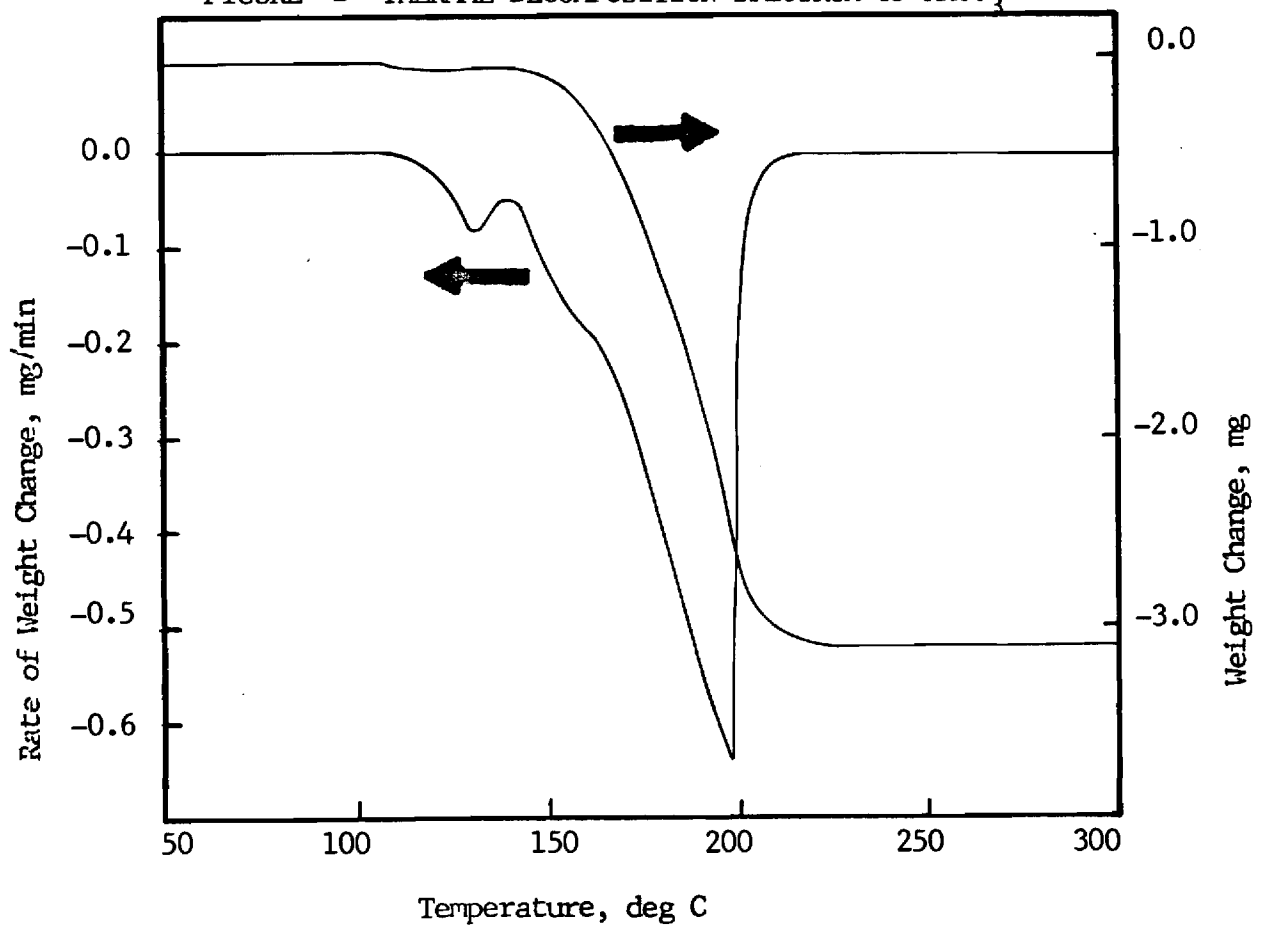

FIGURE 3 RATES OF OXYGEN PRODUCTION vs WATER CONCENTRATION

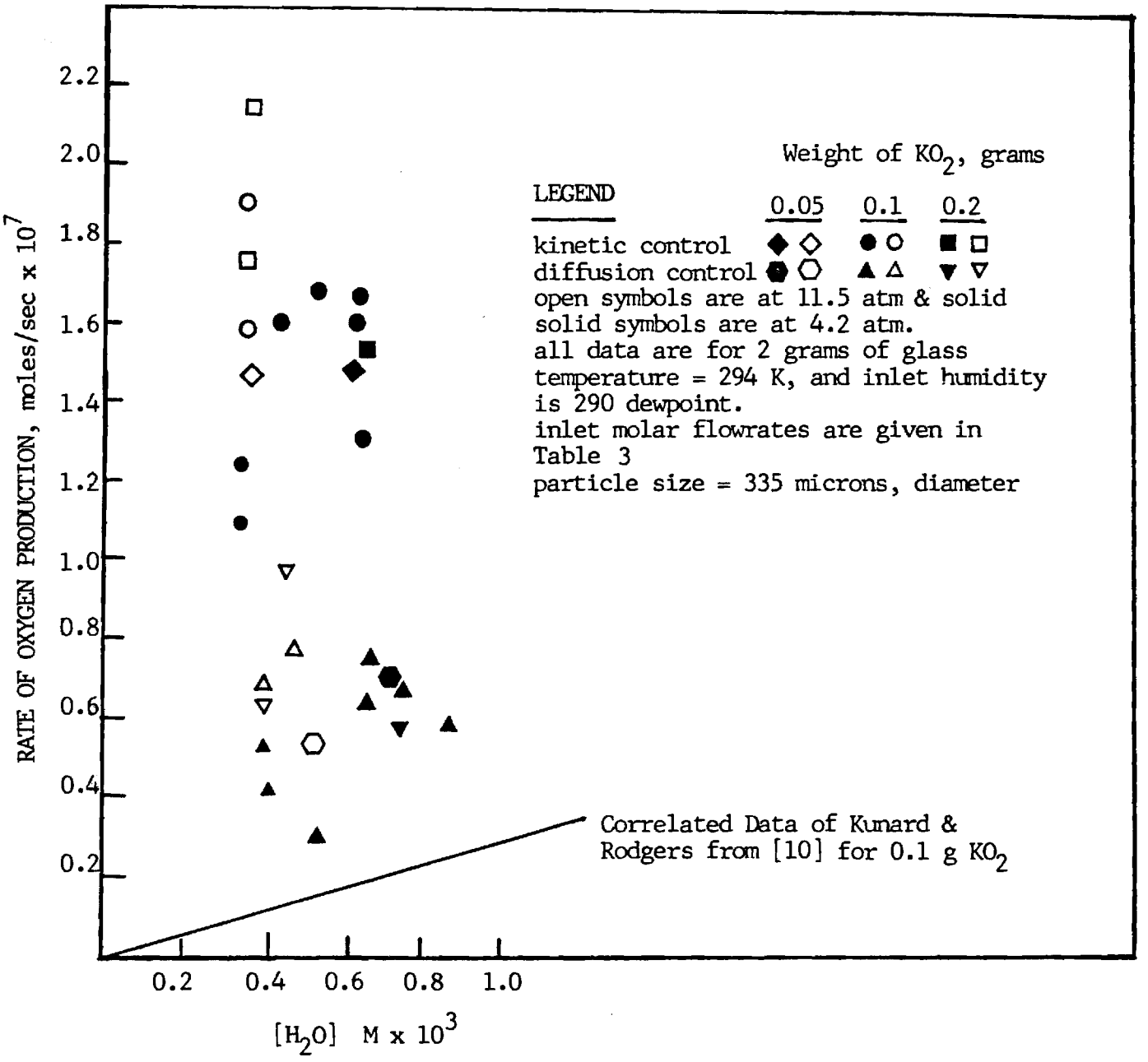

FIGURE 4 SPECIFIC RATES OF OXYGEN PRODUCTION vs WATER CONCENTRATION

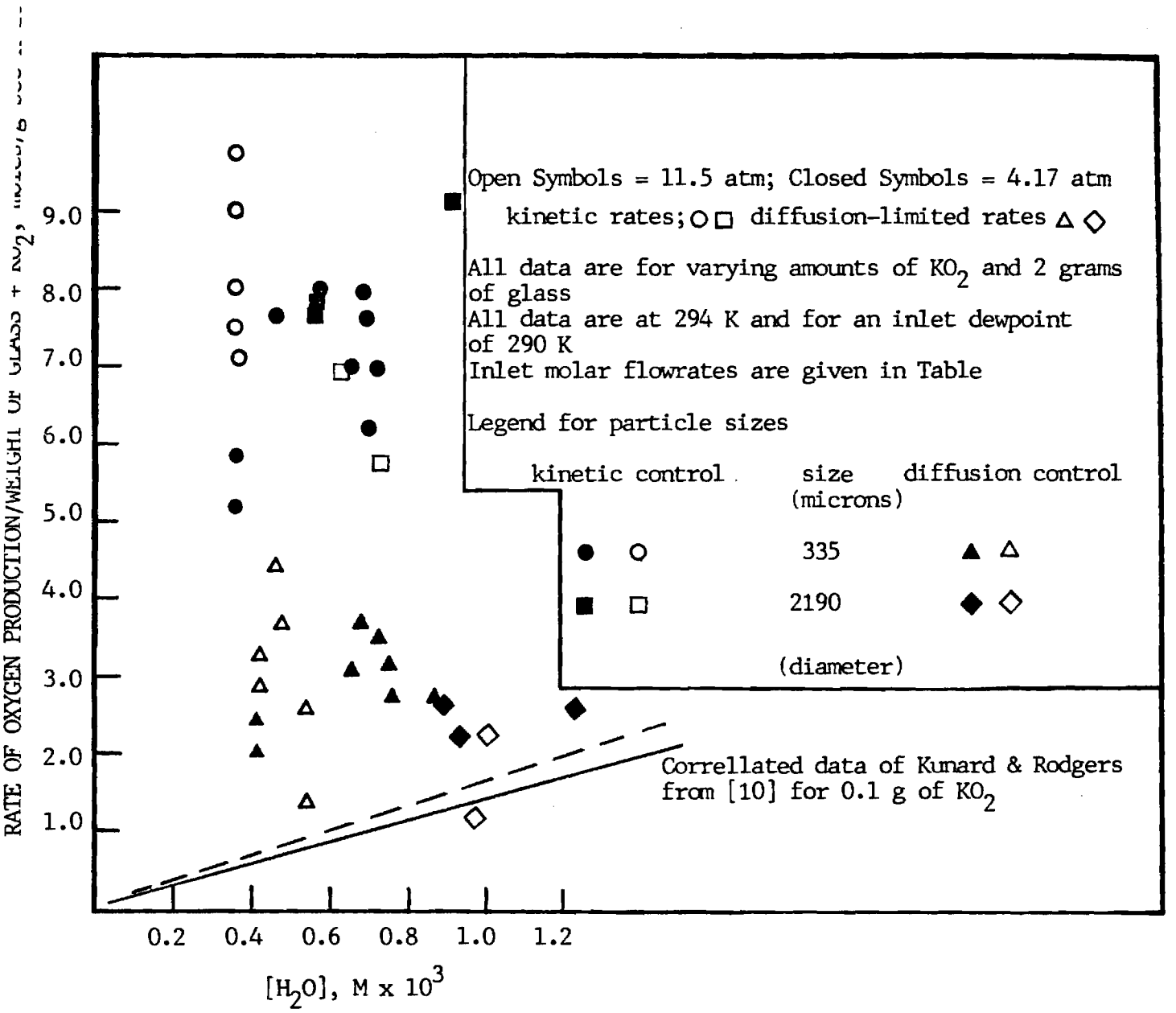

FIGURE 5 TRACE OF OXYGEN CONCENTRATION vs TIME ON STREAM FOR THE BERTY REACTOR AT 4.17 ATM AND ROOM TEMPERATURE

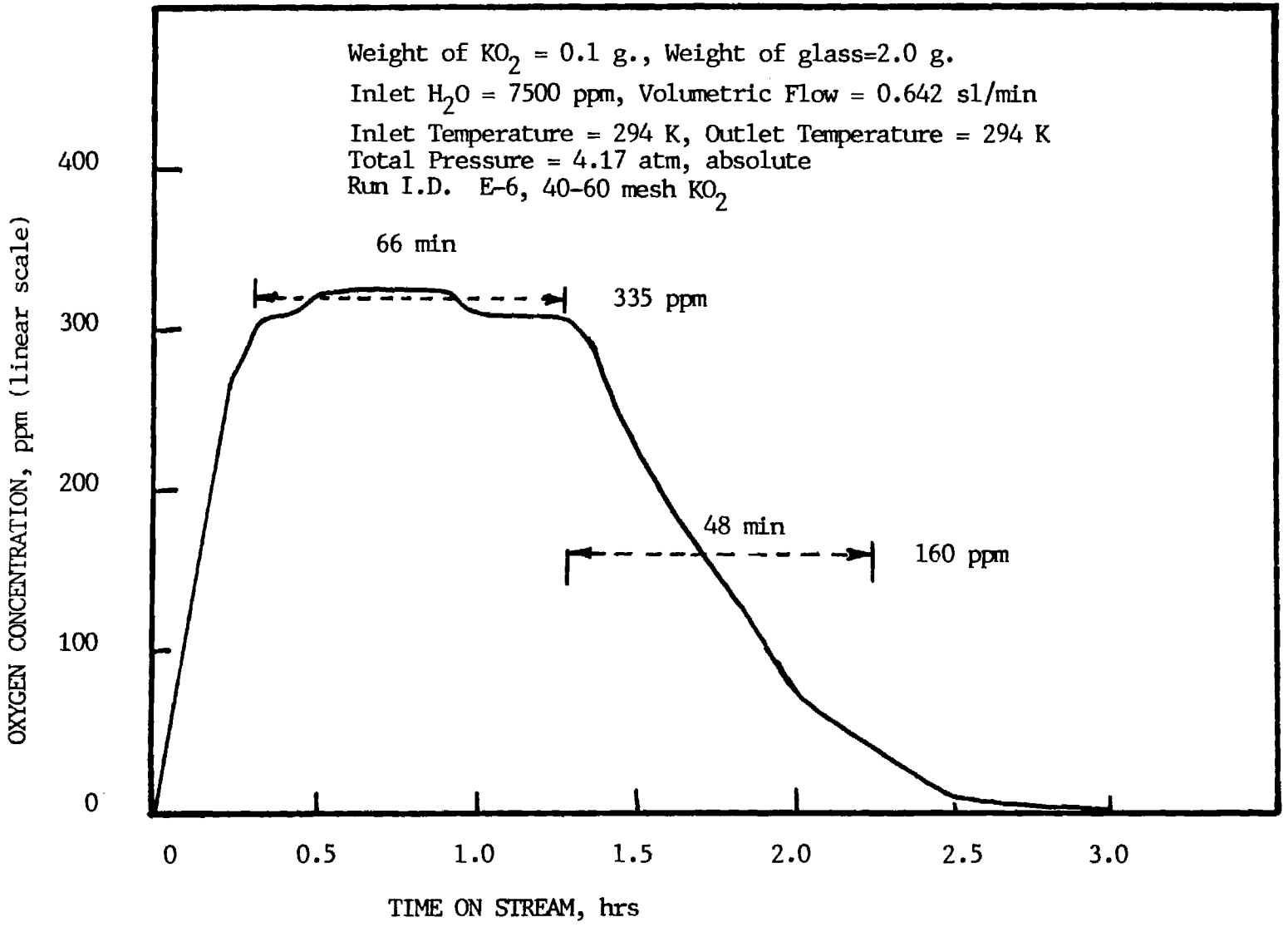

FIGURE 6 TRACE OF OXYGEN CONCENTRATION vs TIME ON STREAM FOR THE BERTY REACTOR AT 11.5 ATM AND ROOM TEMPERATURE

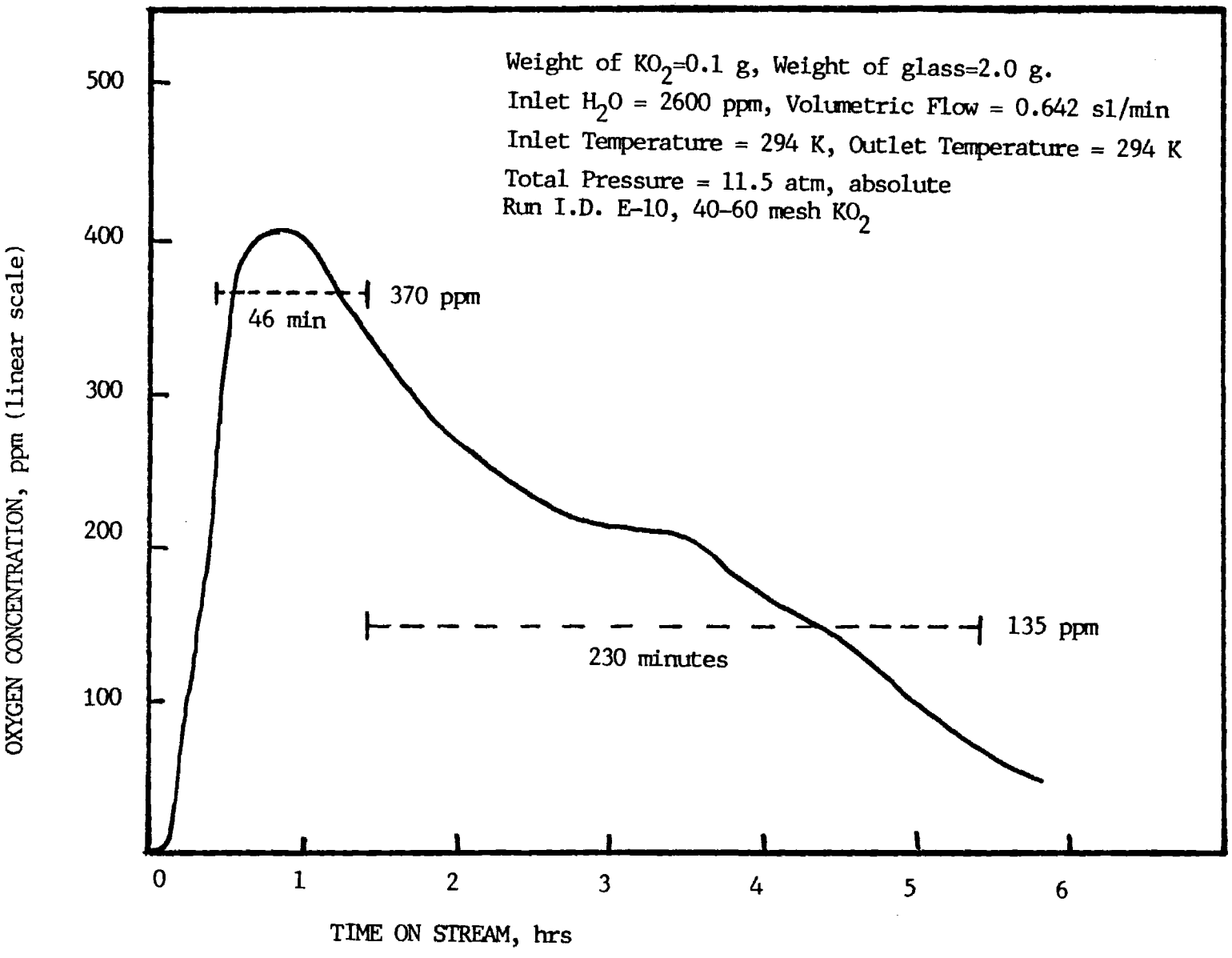

FIGURE 7 TRACE OF OXYGEN CONCENTRATION vs TIME ON STREAM FOR THE PIPE FLOW REACTOR AT 4.17 ATM AND ROOM TEMPERATURE

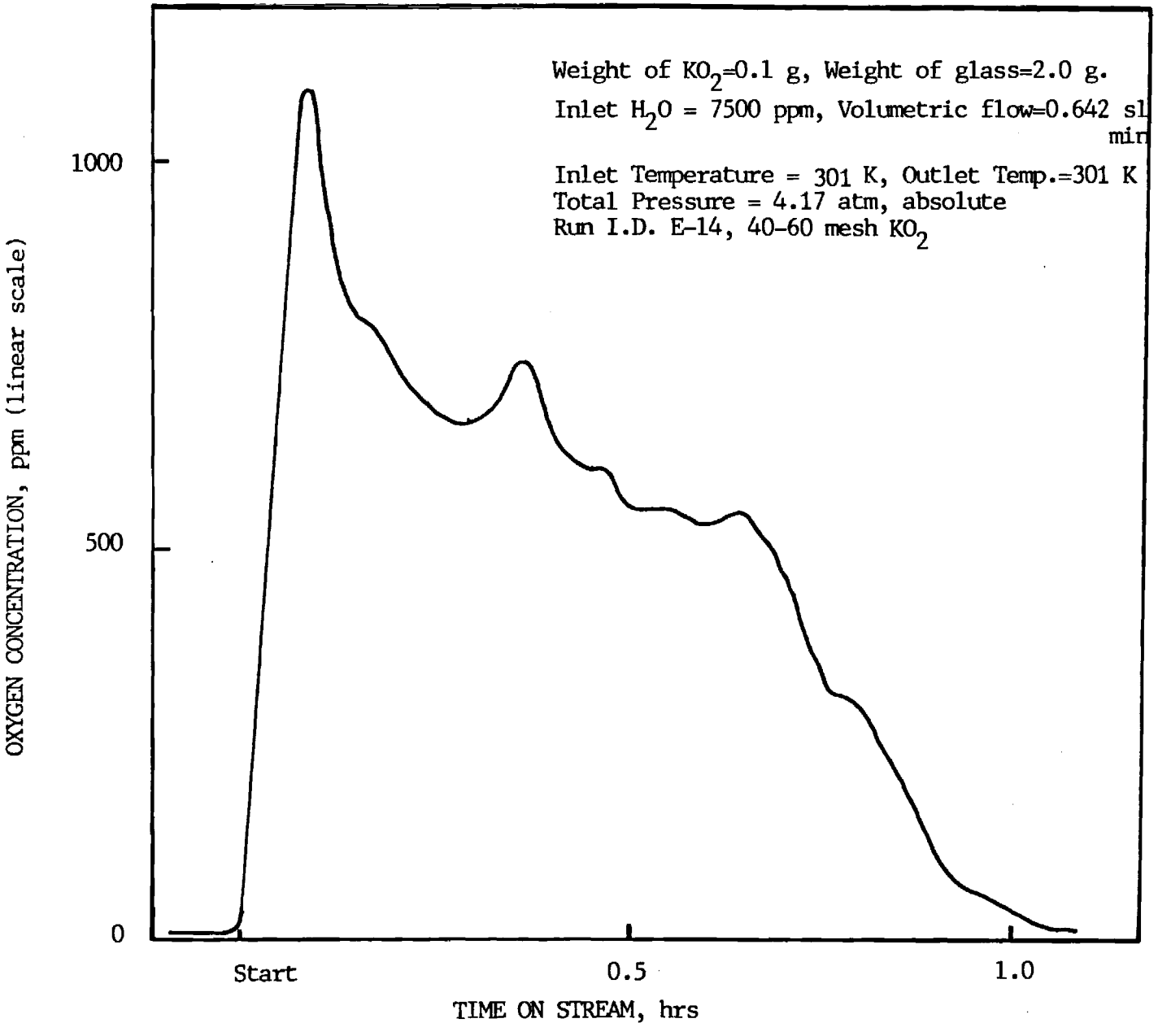

FIGURE 8 TRACE OF WATER CONCENTRATION vs TIME ON STREAM FOR THE PIPE FLOW REACTOR AT 4.17 ATM AND ROOM TEMPERATURE

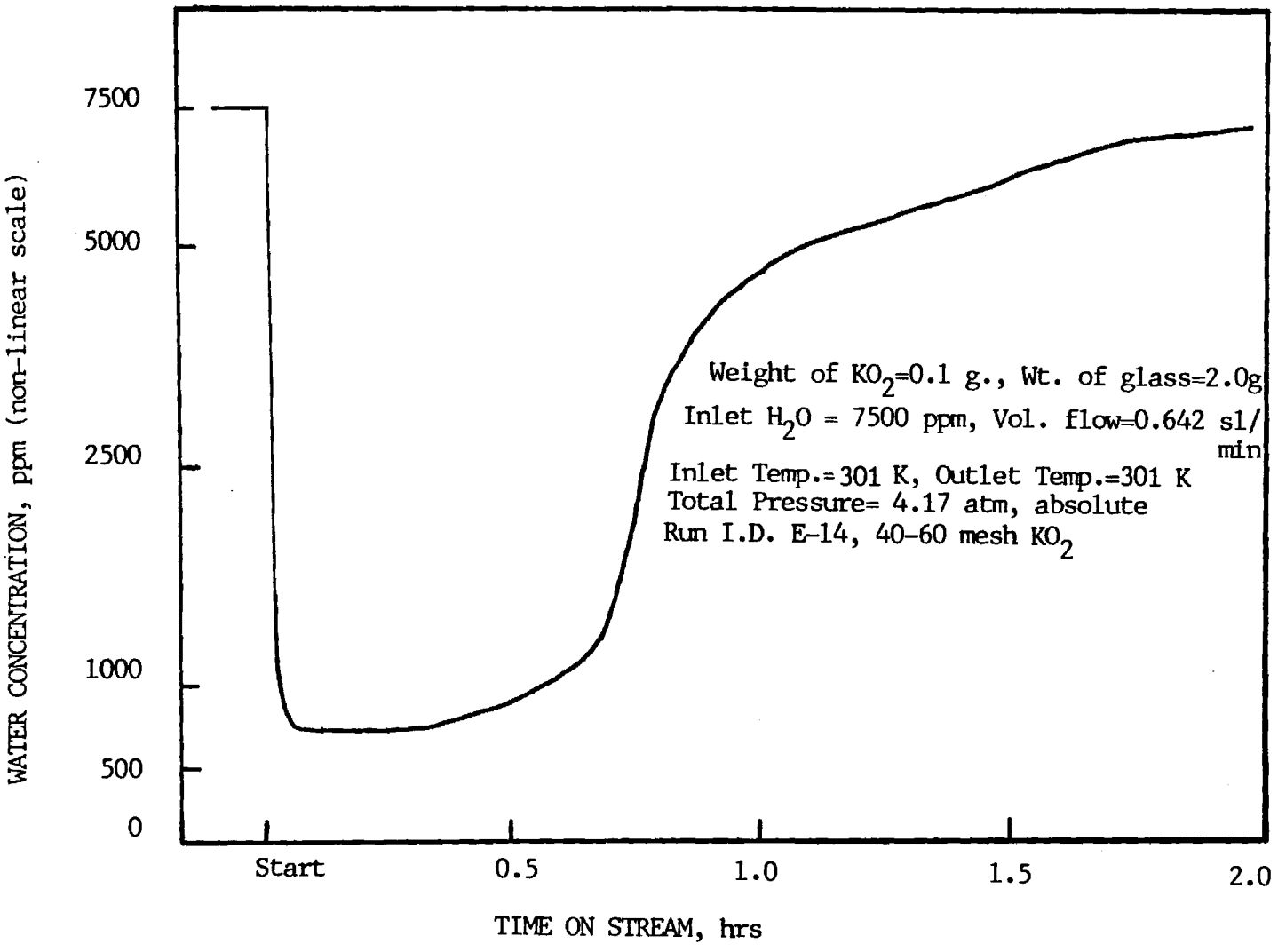

FIGURE 9 TRACE OF OXYGEN CONCENTRATION vs TIME ON STREAM FOR THE PIPE FLOW REACTOR AT 11.5 ATM AND ROOM TEMPERATURE

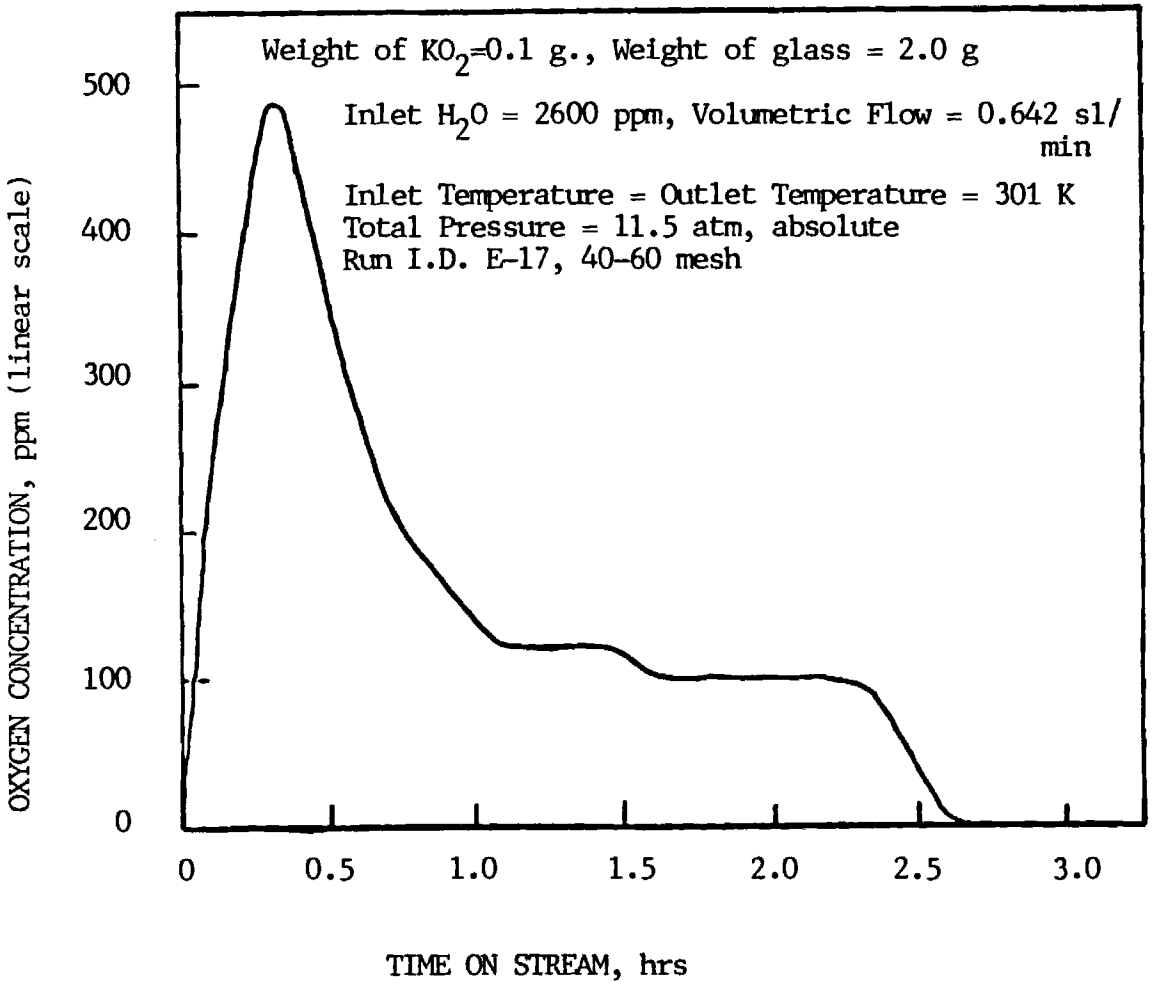

FIGURE 10 TRACE OF WATER CONCENTRATION vs TIME ON STREAM FOR THE PIPE FLOW REACTOR AT 11.5 ATM AND ROOM TEMPERATURE

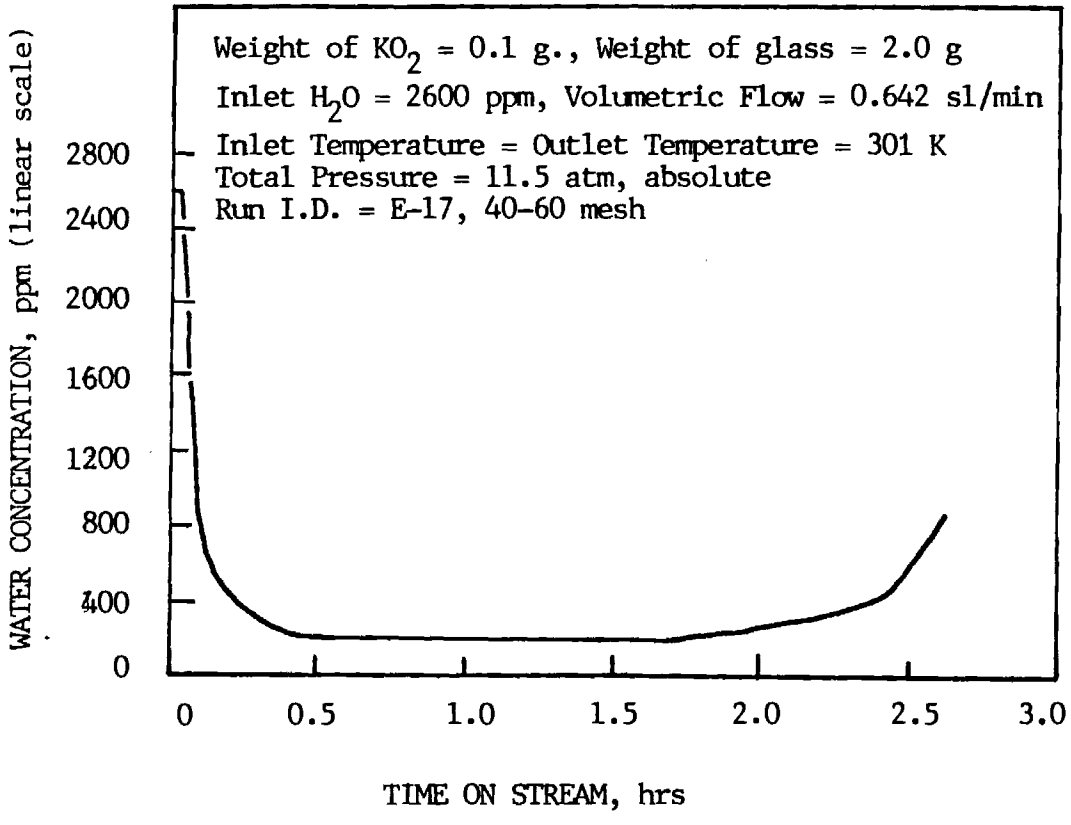

FIGURE 11 TRACE OF WATER CONCENTRATION vs TIME ON STREAM IN THE BERTY REACTOR
EFFECT OF PARTICLE SIZE AT 4.17 ATM

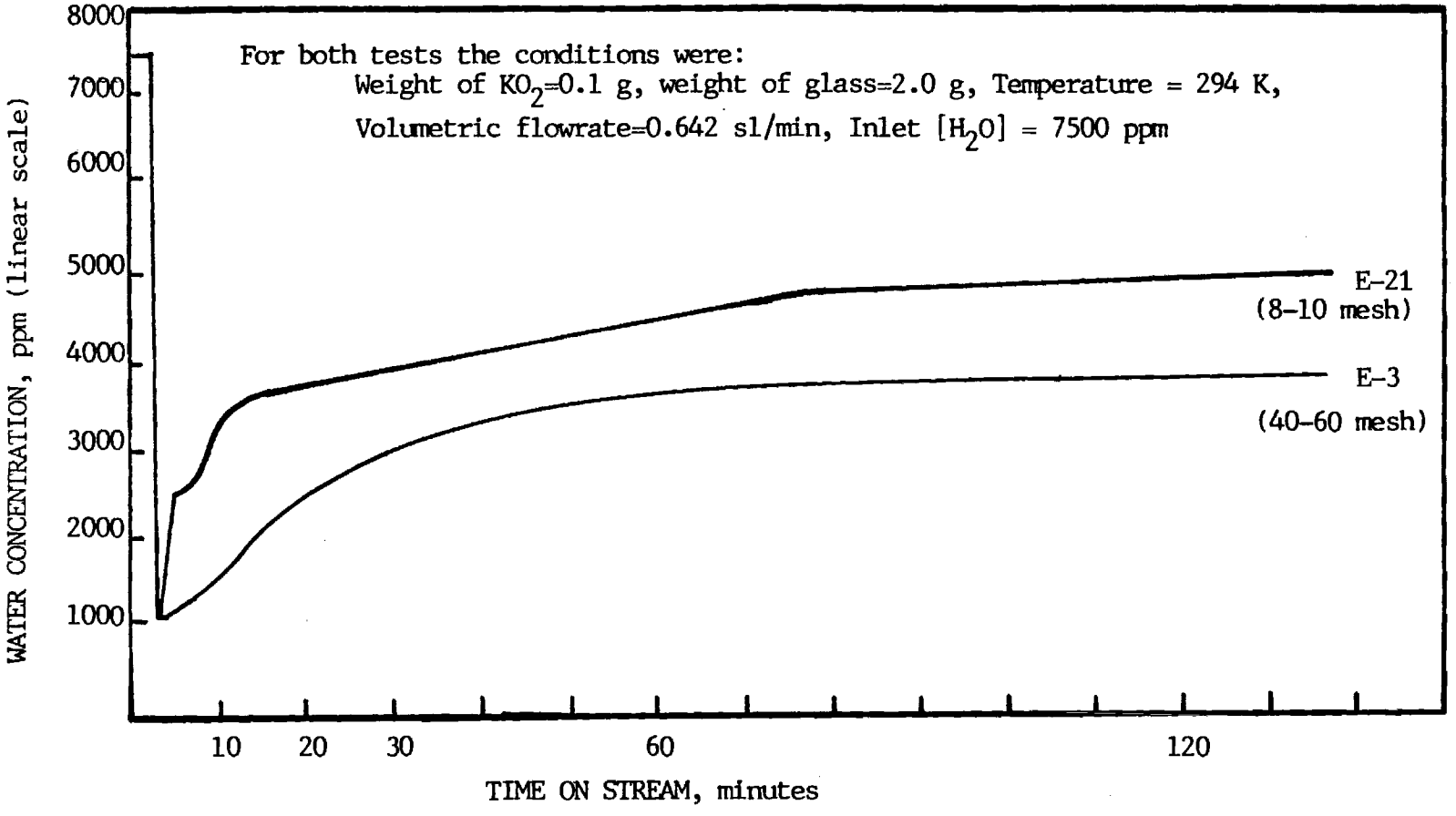

FIGURE 12 TRACE OF OXYGEN CONCENTRATION vs TIME ON STREAM IN THE BERTY REACTOR: EFFECT OF PARTICLE SIZE AT 4.17 ATM

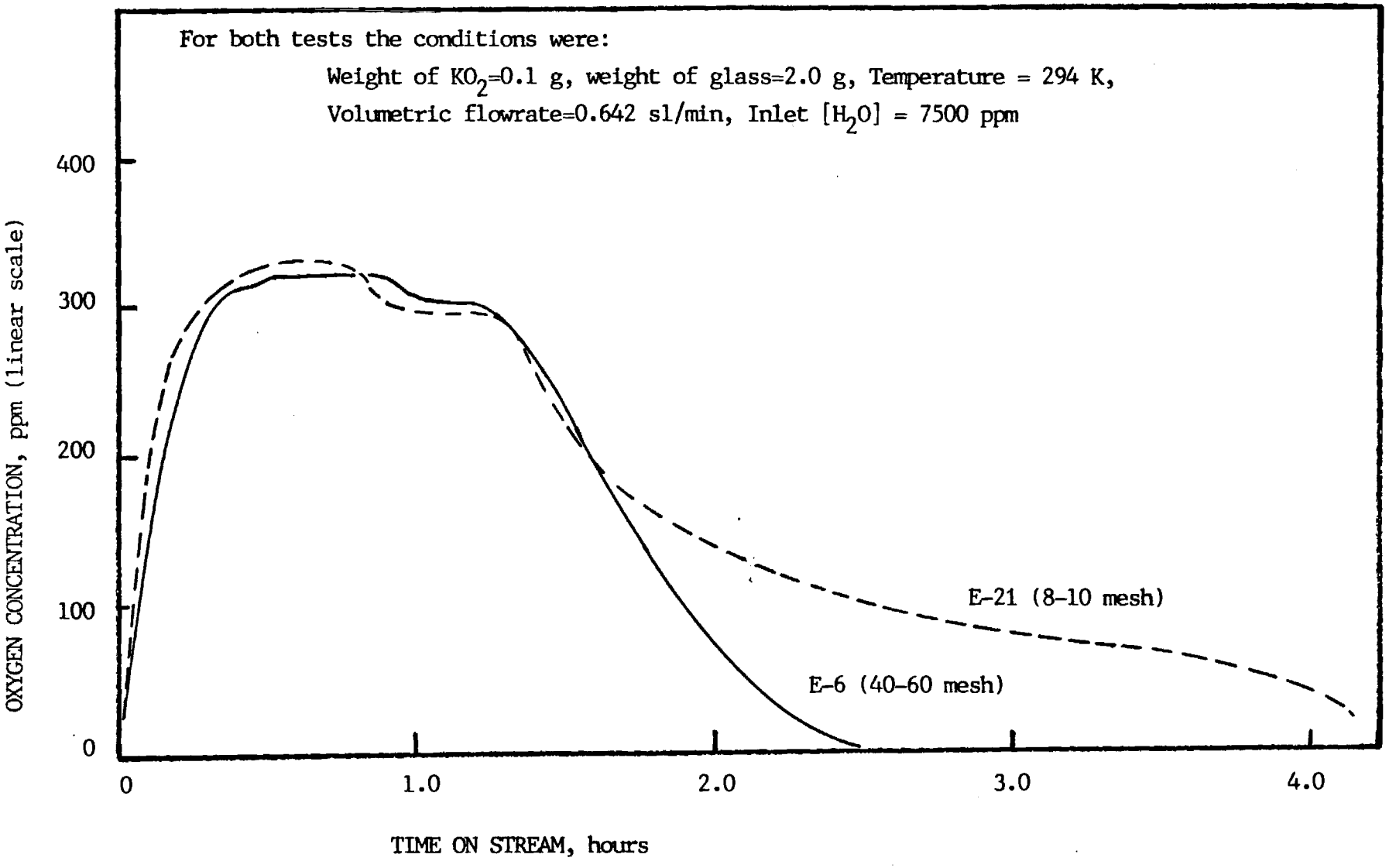

FIGURE 13 EFFECTIVE DIFFUSIVITY OF THE KO_2 USING THE SHRINKING CORE MODEL TO DETERMINE THE PARAMETER